Available online at www.sciencedirect.com
SCIENCE DIRECT®
Journal of Solid State Chemistry 177 (2004) 714–720
JOURNAL OF SOLID STATE CHEMISTRY
http://elsevier.com/locate/jssc

Novel rare-earth-containing manganites $Ba_4REMn_3O_{12}$ (RE = Ce, Pr) with 12R structure

Antonio F. Fuentes,[a] Khalid Boulahya,[b] and Ulises Amador[c,*]

[a] CINVESTAV-IPN Unidad Saltillo, Apartado Postal 663, 25000-Saltillo, Coahuila, Mexico
[b] Departamento de Química Inorgánica, Facultad de Ciencias Químicas, Universidad Complutense, 28040-Madrid, Spain
[c] Departamento de Ciencias Químicas, Facultad de Ciencias Experimentales y de la Salud, Universidad San Pablo-CEU, Urbanización Montepríncipe, 28668-Boadilla del Monte, Madrid, Spain

Received 26 June 2003; received in revised form 15 August 2003; accepted 20 August 2003

Abstract

Novel rare-earth-containing manganites, $Ba_4REMn_3O_{12}$ (RE = Ce, Pr), with 12R structure, have been prepared by solid-state reaction. Although the phases are formed at 950°C, to obtain single-phase samples high temperatures (up to 1300°C) and long synthesis periods are needed.

Their structure is built up from chains of BO_6 face-sharing and corner-sharing octahedra running along the c-axis giving a quasi-one-dimensional oxide. Every polyhedral column consists of (Mn_3O_{12}) units of three face-sharing octahedra, both ends connected by the three terminal oxygen atoms to three different (REO_6) octahedra. Mixed occupation of the three octahedral positions in the structure, (Mn(1), Mn(2) and Re), was not found. Vacancies are not observed, neither in the cationic sublattice nor in the oxygen one. Thus, as in all the other 1-D manganites, the oxidation state of manganese ions seems to be four, as the rare-earth valence is. High-resolution electron microscopy suggests the eventual existence of ordered polytypes for different compositions, which could be stabilized by adjusting the thermodynamic conditions.

Keywords: Manganites; 1-D structure; Rare-earth complex oxides; SAED; HREM

1. Introduction

Complex manganese oxides have attracted the attention of many research groups for decades because of their interesting properties. Among these oxides there are materials for lithium batteries [1,2], magnetic materials [3] and porous materials with catalytic properties [4]. More recently much work has been done on manganites derived from the three-dimensional perovskite $La_{1-x}Ca_xMnO_3$ [5] due to its colossal magnetoresisting (CMR) properties. In the search for new CMR materials some efforts have been devoted to manganites of lower dimensionality: 2-D-Rudelsden–Popper oxides [6] and quasi-one-dimensional compounds, in which MnO_6 octahedra share not only corners but also faces [7]. In this connection the substitution of manganese by a cation of different size and valence in the 1-D oxides 4H-$SrMnO_3$ and 2H-$BaMnO_3$ could be suitable to generate new derivatives, since it may contribute to change the valence of manganese ions, their coordination and also the oxygen stoichiometry. Several 1D-manganites are obtained according to this idea. Besides, they can be doped to give compounds with more complex compositions, such as $Ca_3A'MnO_6$ (A' = Zn, Cu, Co, Ni), $Ba_6A'Mn_4O_{15}$ (A' = Zn, Cu, Co, Ni, Mg, Pd), $Ba_7PdMn_5O_{18}$ and $Sr_4A'Mn_2O_9$ [8]. In this connection, the substitution of calcium (alkaline-earth) [9,10] or of a trivalent cation as In^{3+} [11] for manganese in $BaMnO_{3-x}$, has allowed the stabilization of a new and structurally more complex family of hexagonal perovskite derivatives. In particular, two members of the series $Ba_{5+n}Ca_2Mn_{3+n}O_{3n+14}$ with n = 2 and 3 were stabilized whose structures correspond to the 21R ([$hhccc'cc$]$_3$ sequence) and the 16H ([$hhhccc'cc$]$_2$ sequence) polytypes, respectively. On the other hand, the $Ba_{12}In_3Mn_9O_{34.5}$ oxide shows a structure related to the 12R polytype ([$hhcc$]$_3$ sequence).

To induce a mixed valence state of manganese, common to many of the CMR materials, doping with

*Corresponding author. Fax: +91-351-04-75.
E-mail address: uamador@ceu.es (U. Amador).

0022-4596/$ - see front matter © 2003 Elsevier Inc. All rights reserved.
doi:10.1016/j.jssc.2003.08.025

lanthanide elements is accomplished in RP manganites such as $Sr_{3-x}RE_xMn_2O_7$ [12]. Although doping of one-dimensional hexagonal 4*H*-SnMnO3 and 2*H*-BaMnO3 with lanthanide is feasible, cubic distorted perovskites are obtained [13]. However, many lanthanide-doped 1D oxides have been reported, most of them being ruthenates with 6*H* structure [14]. Interestingly enough, to our best knowledge, the only mixed-valence manganite in which MnO_6 octahedra share faces, is the lanthanide-containing 1D oxide $Ba_3ErMn_2O_9$ [15] with 6*H* structure.

Bearing in mind this information, we have studied the effects of various substitutions of manganese by cerium and praseodymium in the $BaMnO_{3-x}$ system.

2. Experimental section

Polycrystalline samples of different compositions in the system Ba–Mn–*RE*–O (*RE* = Ce, Pr) have been prepared by standard solid-state reaction. Starting chemicals used in this work were $BaCO_3$ (Aldrich Chem. Co., Inc. 99.8%), MnO_2 (Aldrich Chem. Co., Inc. 99 + %), CeO_2 (Aldrich Chem. Co., Inc. 99.9%) and Pr_6O_{11}. Freshly prepared praseodymium oxide, Pr_6O_{11}, was obtained after firing $Pr(NO_3)_3 \cdot 6H_2O$ (Aldrich Chem. Co., Inc. 99 + %) 12 h at 800°C. Stoichiometric amounts of these starting reagents were intimately mixed in an agate mortar under acetone and the resulting powder was heated in air in high alumina crucibles (Adolph Coors, Co.) at 950°C for 12 h in order to decompose the carbonate. The powders were then uniaxially pressed into 12 mm diameter pellets and fired in air, at several temperatures ranging from 1100°C to 1300°C for different holding times followed by natural furnace cooling to room temperature. One week was the total firing time for each composition with regular regrinding and repelleting to ensure complete reaction. The progress of reaction was followed by X-ray powder diffraction (XRD) on a Philips X'Pert diffractometer equipped with Cu($K\alpha1 + \alpha2$) radiation ($\lambda = 1.5418$ Å) and a nickel filter.

The XRD patterns used for structure determination were obtained on a Bruker D8 diffractometer of Bragg–Bentano geometry, equipped with a graphite primary monochromator giving a monochromatic beam of Cu($K\alpha1$) radiation ($\lambda = 1.5406$ Å). These patterns were collected at room temperature from 15° to 95° (2θ) using a step size of 0.02° obtaining 4000 points and about 1600 reflections. The data were analyzed by the Rietveld method using the FULLPROF program [16]; the fitting process was finished when convergence was reached.

Selected area electron diffraction (SAED) and high-resolution electron microscopy (HREM) were performed on a PHILIPS CM200 FEG electron microscope, fitted with a double tilting goniometer stage ($\pm 40°$, $\pm 24°$). Local composition was analyzed with an EDAX analyzer system attached to the above microscope. Simulated HREM images were calculated by the multislice method using the MacTempas software package.

3. Results and discussion

3.1. Synthesis

Several samples of different compositions were prepared in the Ba–Ce–Mn–O system with CeO_2/MnO_2 molar ratios: 1/5 ($Ba_6CeMn_5O_{18}$), 1/4 ($Ba_5CeMn_4O_{15}$), 1/3 ($Ba_4CeMn_3O_{12}$), 1/2 ($Ba_3CeMn_2O_9$) and 1/1 (Ba_2CeMnO_6); all of them on the line of the phase diagram connecting $BaCeO_3$ and $BaMnO_3$.

Powder X-ray diffraction patterns of the samples obtained from the initial mixtures treated at 950°C (not shown) revealed the formation of a new compound which is the major phase for the composition $4BaCO_3$: CeO_2: $3MnO_2$ of the reacting mixture. Thus, we have studied this sample more deeply. The powder was subjected to further firings at increasing temperatures (up to 1300°C) until complete removal of undesired phases or until no changes were observed in the diffraction patterns collected after two consecutive thermal treatments. Fig. 1 shows the X-ray diffraction pattern of the obtained $Ba_4CeMn_3O_{12}$ sample. The whole pattern can be indexed with a rhombohedral unit cell of parameters $a = 5.7980(1)$ Å and $c = 28.6070(8)$ Å; a small amount of CeO_2 (about 6% weight) is observed as an impurity. The praseodymium-containing analog must be prepared at slightly lower temperatures, about 1250°C, to avoid its decomposition. Fig. 2 shows the X-ray diffraction pattern of the $Ba_4PrMn_3O_{12}$ sample. The whole pattern can be indexed with a rhombohedral unit cell of parameters $a = 5.7943(1)$ Å and $c = 28.5716(3)$ Å; in this case a small amount (about 5% weight) of Pr_6O_{11} is observed as an impurity.

It is not evident why some rare-earth oxides are observed as an impurity in both samples; this is, most likely, due to the formation of a small quantity of any of the $BaMnO_{3-x}$ oxides. Most of these oxides are difficult to identify because of their structural similarity with the title compounds [17].

3.2. Preliminary structural characterization

Selected area electron diffraction (SAED) has been used to fully reconstruct the reciprocal space of both, $Ba_4CeMn_3O_{12}$ and $Ba_4PrMn_3O_{12}$ materials. All the studied crystals were analyzed by EDS to be sure about their composition; in every case the actual compositions are close to the nominal ones, in spite of the presence in the samples of small amounts of impurity phases.

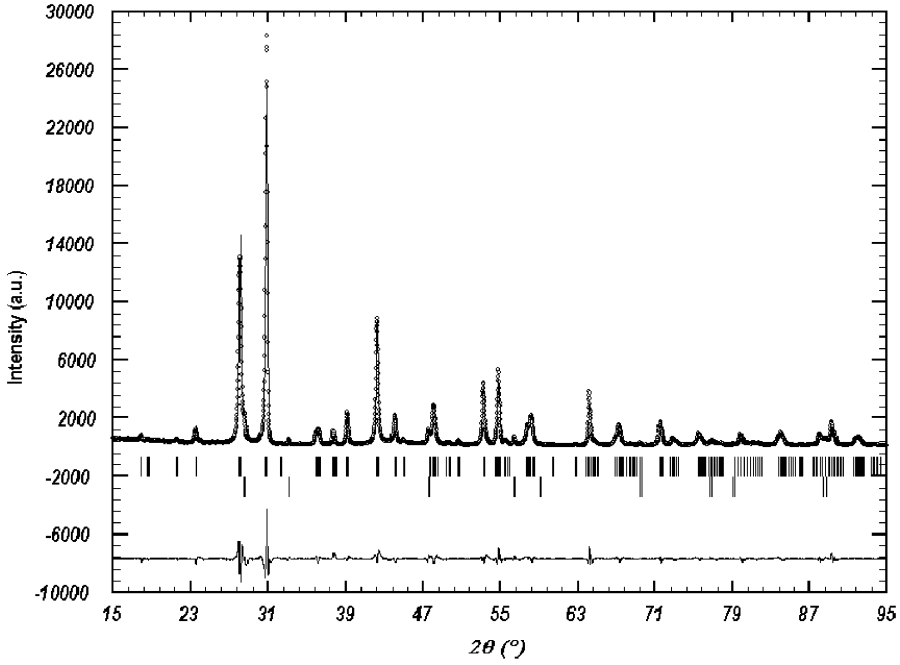

Fig. 1. Graphic results of the fitting of the X-ray powder diffraction data of $Ba_4CeMn_3O_{12}$: experimental (points), calculated (solid line) and difference (bottom). Vertical marks indicate the peaks of the phases present in the sample: first row $Ba_4CeMn_3O_{12}$ and second row CeO_2.

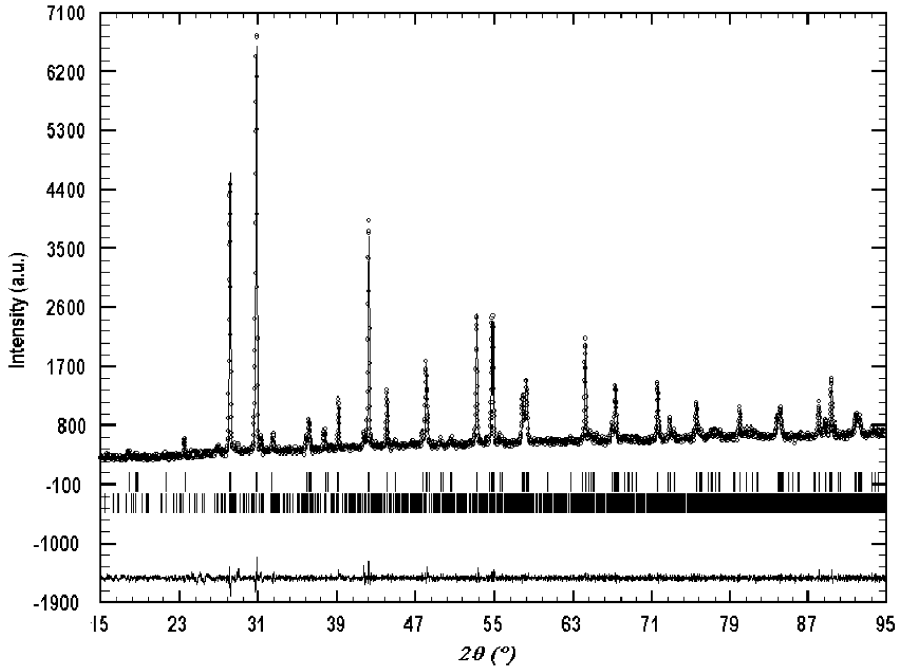

Fig. 2. Graphic results of the fitting of the X-ray powder diffraction data of $Ba_4PrMn_3O_{12}$: experimental (points), calculated (solid line) and difference (bottom). Vertical marks indicate the peaks of the phases present in the sample: first row $Ba_4CeMn_3O_{12}$ and second row Pr_6O_{11}.

Microstructural characterization of $Ba_4CeMn_3O_{12}$ by SAED and HREM confirms the XRD results. The most relevant reciprocal zone axis, [010], is shown in Fig. 3a. The diffraction maxima can be indexed with a rhombohedral unit cell of parameters $a = 5.8$ Å and $c = 28.6$ Å. Reflection conditions for this phase ($h00$: $h = 3n$, $00l$: $l = 3n$ and hkl: $-h + k + l = 3n$) are compatible with the space group $R\bar{3}m$ (166). The corresponding HREM micrograph (Fig. 3b) shows an apparently well-ordered material with d-spacings of 4.9 and 28.6 Å, corresponding

to d_{100} and d_{001}. The structure can be directly revealed from the contrast observed in this image: the bright dots correspond to rows of Ba and Ce atoms. From the Ba distribution this contrast can be interpreted as a $(hhhc)_3$ stacking sequence which is isotypic to that observed in $Ba_4ZrRu_3O_{12}$ [18]. Therefore, from the refined atomic parameters of $Ba_4CeMn_3O_{12}$ (see the next section), an image calculation was performed. The simulated image fits nicely to the experimental one at $\Delta t = 30$ Å and $\Delta f = -650$ Å.

We have also performed a SAED and HREM study of the sample with Ce to Mn ratio of 1/4, i.e., of formal composition $Ba_5CeMn_4O_{15}$. The main feature, common to all the examined crystals, is the presence of a clear structural disorder. The reciprocal zone axis [010], is shown in Fig. 4a. The corresponding HREM (Fig. 4b) shows that the basal plane (a, b) is apparently well ordered, but along the c-axis a disordered inter-growth of phases with variable number (n) of octahedral is observed, as marked with arrows on the micrograph. The unit-cell parameters of those hypothetical phases (polytypes) can be expressed as $a = 5.8$ Å and $c = n \times 2.38$ Å (2.38 Å being the distance between two consecutive octahedra along the c-axis). Two important conclusions can be obtained from the formation of this complex scheme of inter-growth. First, this mechanism allows the sample to accommodate a cationic composition (a Ce/Mn ratio) for which a stable ordered structure is not favored in the thermodynamic conditions applied. This kind of complex microstructure is also found in other similar systems [19,20]. Secondly, this suggests the eventual existence of ordered polytypes for different compositions. Thus, with the adequate composition by adjusting the thermodynamic conditions (temperature, oxygen pressure, hydrostatic pressure, etc.) it would be possible to prepare single-phase samples of those polytypes. In particular, Fig. 4b suggests the existence of phases with compositions $Ba_6CeMn_5O_{18}$ (sequence along the c-axis corresponding to $n = 6$ or an entire multiple), $Ba_4CeMn_3O_{12}$ ($n = 4$, which is the title compound) and $Ba_5CeMn_4O_{15}$ (which is the nominal composition of the sample with, corresponding to sequences along the c-axis of an entire multiple of five octahedra). Works are in progress to stabilize these polytypes.

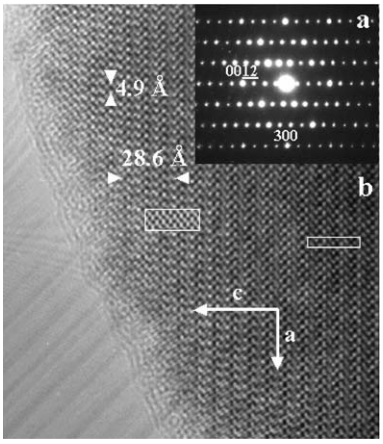

Fig. 3. (a) SAED pattern of $Ba_4CeMn_3O_{12}$ along [010]. (b) Corresponding HRTEM image; simulated images are shown in the insets.

The praseodymium-containing manganite, $Ba_4PrMn_3O_{12}$, was also studied by selected area electron diffraction (SAED). The actual composition of every crystal was determined by EDS to be consistent with the nominal composition of the sample. The most relevant reciprocal zone axis, [010], is shown in Fig. 5a. This phase was found to be isostructural with $Ba_4CeMn_3O_{12}$,

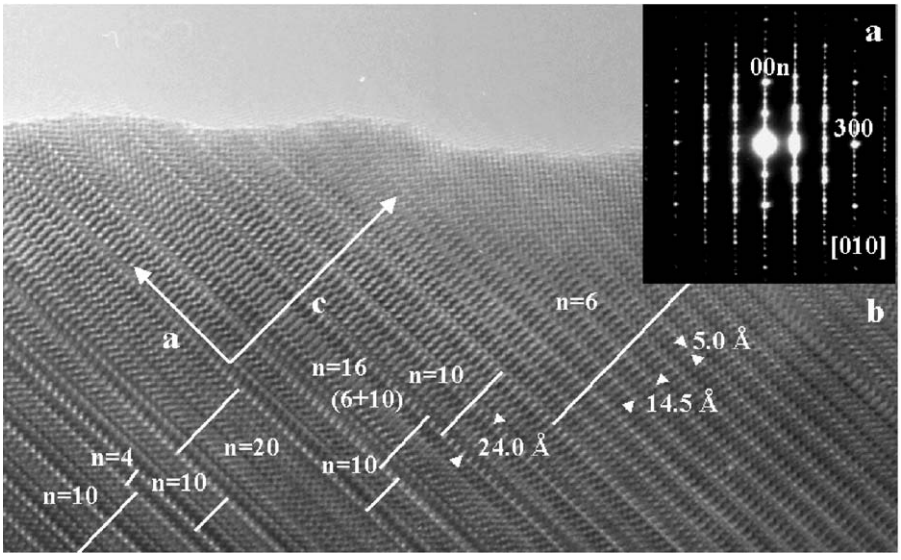

Fig. 4. (b) SAED pattern of "$BaCeMnO_{15}$" sample along [010]. (b) Corresponding HRTEM image.

all the diffraction pattern being indexed with a rhombohedral unit cell of parameters $a=5.8$ Å and $c=28.7$ Å, in agreement with the XRD results. The corresponding HREM micrograph (Fig. 5b) shows an apparently well-ordered material with *d*-spacings of 4.9 and 28.6 Å, corresponding to d_{100} and d_{001}. The simulated image performed using the refined atomic co-ordinates fits nicely to the experimental one at $\Delta t=25$ Å and $\Delta f=-550$ Å.

3.3. Structure refinement

Since the previous structural results, obtained from SAED and HREM data, suggested that the title compounds are isostructural with $Ba_4ZrRu_3O_{12}$ [18], the structure of the latter was used as starting model for the fitting of the XRD data of $Ba_4REMn_3O_{12}$ (*RE*=Ce, Pr). Figs. 1 and 2 show the graphic result of the fitting of the experimental X-ray diffraction patterns for $Ba_4CeMn_3O_{12}$ and $Ba_4PrMn_3O_{12}$, respectively and the difference between the observed and the calculated data. The final structural parameters are collected in Table 1 whereas Table 2 shows some selected inter-atomic distances. In Fig. 6 a schematic representation of the structure is depicted. It is worth pointing out, that the structure refinement of this type of one-dimensional oxides presents some serious problems, such as a strong preferred orientation effect due to the pronounced hexagonal shape of the crystallites. Another important point to be considered is the relatively weak scattering factor of oxygen atoms when compared to heavy atoms such as Ba, Mn and Ce (or Pr). In spite of this, the refinements were stable and it was possible to refine the structural parameters of the oxygen atoms, including the isotropic temperature factors.

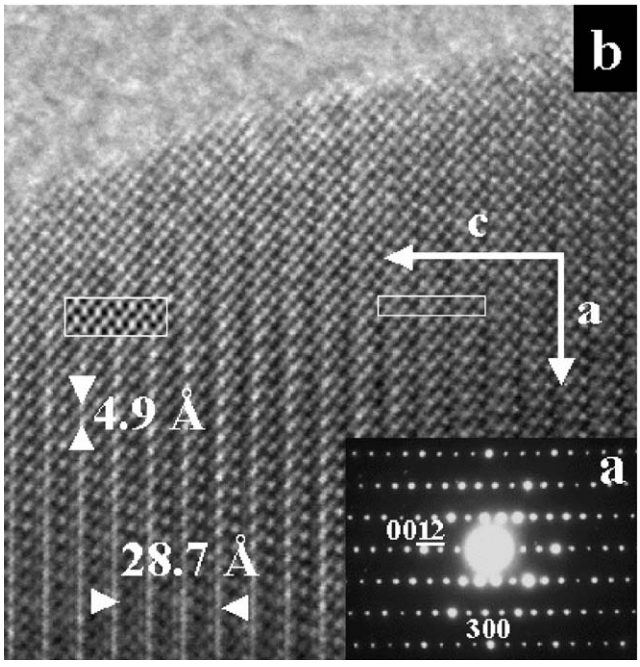

Fig. 5. (a) SAED pattern of $Ba_4PrMn_3O_{12}$ along [010]. (b) Corresponding HRTEM image; simulated image is shown in the inset.

The structure of the title compounds is built up from chains of BO_6 face-sharing and corner-sharing octahedra running along the *c*-axis giving a quasi-one-dimensional oxide. Every polyhedral column consists of (Mn_3O_{12}) units of three face-sharing octahedra, both ends connected by the three terminal oxygen atoms to three different (REO_6) octahedra. Mixed occupation of the three octahedral positions in the structure was not found. Thus, manganese ions occupy the 3*b* and 6*c* sites, whereas the *RE* cations occupy the 3*a* sites. Moreover, vacancies are not observed, neither in the cationic sublattice nor in the oxygen one. Thus, within the experimental errors, the refined compositions agree with those determined by EDS, and the manganese and rare-earth ions can be assumed to be in a tetravalent state.

Concerning the bond lengths, in $Ba_4CeMn_3O_{12}$, the two Ba atoms are 12-coordinated by oxygen in very distorted polyhedra, at distances over the range 2.91 to

Table 1
Final structural parameters for $Ba_4CeMn_3O_{12}$ and $Ba_4PrMn_3O_{12}$

Atom site[a]	Ba(1) 6*c*	Ba(2) 6*c*	*M* 3*a*	Mn(1) 3*b*	Mn(2) 6*c*	O(1) 18*h*	O(2) 18*h*
M=Ce; $Ba_4CeMn_3O_{12}$[b]							
x/a	0.0	0.0	0.0	0.0	0.0	0.482(1)	0.488(1)
y/b	0.0	0.0	0.0	0.0	0.0	0.518(2)	0.512(1)
z/c	0.1312(1)	0.2831(1)	0.0	0.5	0.4132(2)	0.1240(4)	0.28890(5)
$B_{iso}(A^2)$	0.54(4)	0.60(5)	0.77(3)	0.32(5)	0.21(4)	0.33(4)	0.51(5)
M=Pr; $Ba_4PrMn_3O_{12}$[c]							
x/a	0.0	0.0	0.0	0.0	0.0	0.497(1)	0.486(1)
y/b	0.0	0.0	0.0	0.0	0.0	0.503(1)	0.514(1)
z/c	0.1309(1)	0.2838(1)	0.0	0.5	0.4144(3)	0.1232(5)	0.2879(6)
$B_{iso}(A^2)$	0.24(2)	0.23(3)	0.29(3)	0.22(2)	0.32(4)	0.67(5)	0.68(4)

[a] SG: $R\bar{3}m$ (166)
[b] For $Ba_4CeMn_3O_{12}$, $a=5.7980(1)$ Å, $c=28.6070(8)$ Å; $V=832.83(4)$ Å^3, $\rho=6.26(1)$ g/cm^3, $R_B=0.046$, $R_{exp}=0.033$, $R_{wp}=0.051$, $\chi^2=2.4$
[c] For $Ba_4PrMn_3O_{12}$, $a=5.7943(1)$ Å, $c=28.5716(3)$ Å; $V=830.76(1)$ Å^3, $\rho=6.28(1)$ g/cm^3, $R_B=0.020$, $R_{exp}=0.041$, $R_{wp}=0.048$, $\chi^2=1.3$

Table 2
Selected inter-atomic distances less than 3.5 Å in $Ba_4CeMn_3O_{12}$ and $Ba_4PrMn_3O_{12}$

$Ba_4CeMn_3O_{12}$		$Ba_4PrMn_3O_{12}$	
Ba(1)–O(1)	2.912(6) × 6	Ba(1)–O(1)	2.906(8) × 6
Ba(1)–O(1)^{i}	2.908(8) × 3	Ba(1)–O(1)^{I}	2.83(1) × 3
Ba(1)–O(2)	3.064(9) × 3	Ba(1)–O(2)	3.04(1) × 3
Average	2.949(8)	Average	2.922(3)
Ba(2)–O(1)	2.812(9) × 3	Ba(2)–O(1)	2.71(1) × 3
Ba(2)–O(2)	2.906(6) × 6	Ba(2)–O(2)	2.903(8) × 6
Ba(1)–O(2)^{i}	3.12(1) × 3	Ba(1)–O(2)^{I}	3.12(1) × 3
Average	2.936(9)	Average	2.907(3)
Ce–O(2)	2.20(1) × 6	Pr–O(2)	2.23(1) × 6
Mn(1)–O(1)	1.926(8) × 6	Mn(1)–O(1)	2.06(1) × 6
Mn(2)–O(1)	1.952(9) × 3	Mn(2)–O(1)	2.04(1) × 3
Mn(2)–O(2)	1.855(9) × 3	Mn(2)–O(2)	1.84(1) × 3
Average	1.903(9)	Average	1.937(4)
Distortion[a]	6.5×10^{-4}	Distortion[a]	26.1×10^{-4}
Ba(1)–Mn(1)	3.498(1)	Ba(1)–Mn(1)	3.498(1)
Ba(2)–Mn(2)	3.453(2)	Ba(2)–Mn(2)	3.464(2)
Mn(1)–Mn(2)	2.484(6)	Mn(2)–Mn(2)	2.447(8)

[a] Distortion $= 1/n \sum[(d_i - \langle d \rangle)/\langle d \rangle]^2$

3.06 Å for Ba(1); these distances ranging from 2.81 to 3.12 Å for Ba(2). On the other hand, in $Ba_4PrMn_3O_{12}$, the coordination polyhedra of Ba atoms are also very distorted, the barium to oxygen distances ranging from 2.90 to 3.04 Å for Ba(1), and 2.71 to 3.12 Å for Ba(2). All these distances are consistent with previously reported Ba–O distances in comparable 1-D systems [8–11,17].

Manganese ions are located in two different octahedral sites in the structure of $Ba_4CeMn_3O_{12}$ compounds: Mn(1) is located in a larger and regular environment with six equal Mn(1)–O distances of 1.926 Å (Table 2); whereas the $Mn(2)O_6$ octahedra are quite distorted, with three large (1.952 Å) and three short (1.855 Å) Mn(2)–O distances (average 1.903 Å). A similar situation is found in $Ba_4PrMn_3O_{12}$ (Table 2) with slightly larger Mn–O distances. The Mn–O distances (from 1.84 to 2.06 Å) are typical of Mn^{4+} octahedra in an oxide matrix [8–11,17]. As in other manganese oxides containing trimmers of face-sharing octahedra, the MnO_6 octahedron which shares faces with two other MnO_6 octahedra (Mn(1) in these cases), is quite regular whereas the terminal octahedra ($Mn(2)O_6$) are more distorted [21,22]. In the title compounds the distortion of the $Mn(2)O_6$ octahedra is a consequence of the large size of the rare-earth ions ($r(Ce^{+4}(VI)) = 0.80$ Å; $r(Pr^{+4}(VI)) = 0.78$ Å) compared to manganese ions ($r(Mn^{+4}(VI)) = 0.54$ Å) [23]. Indeed, to accommodate the large *RE* ions, the BaO_3 layers are distorted and displaced from their ideal

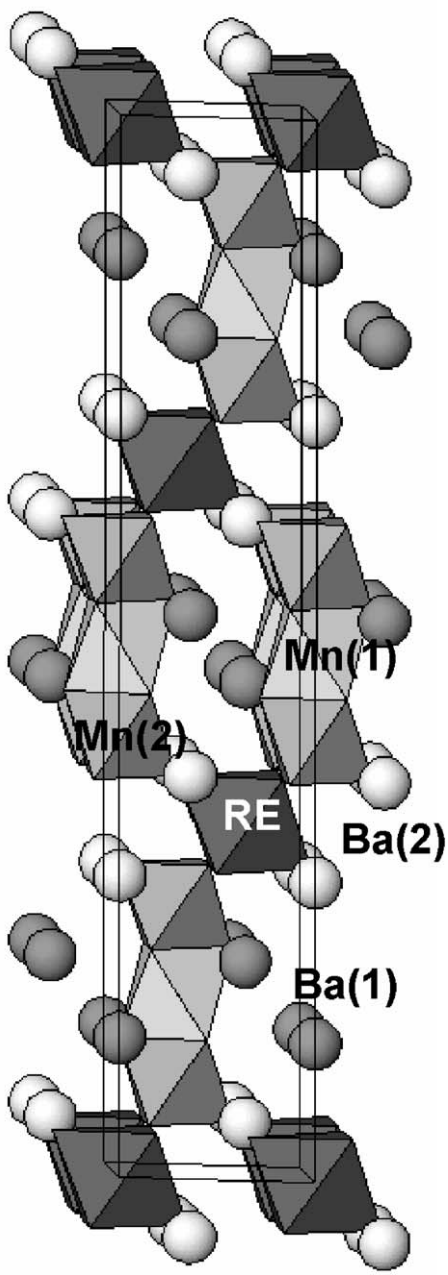

Fig 6. Schematic representation of the structure of $Ba_4REMn_3O_{12}$ (*RE* = Ce, Mn).

positions. Ideally, two consecutive BaO_3 layers in the 12*R* structure should be separated by $c/12 = 2.38$ Å. However, the actual situation in both $Ba_4CeMn_3O_{12}$ and $Ba_4PrMn_3O_{12}$ compounds is more complex. Thus, two consecutive layers built up from Ba(2) and O(2), in between the rare-earth ions are placed, are separated by 2.87 Å (distance between the barium atoms of each layer) in the cerium-containing oxide; this distance being 2.83 Å in $Ba_4PrMn_3O_{12}$. These layers are not flat, the oxygen atoms being out of the barium planes by 0.17 Å in $Ba_4CeMn_3O_{12}$; this distortion is 0.12 Å in the

praseodymium-containing analog. The other two distances between BaO_3 layers also deviate from the ideal separation. In $Ba_4CeMn_3O_{12}$ the distance between two consecutive layers containing Ba(1) and O(1), separated by $Mn(1)O_6$ octahedra, is quite short (2.03 Å; 2.05 in $Ba_4PrMn_3O_{12}$) despite the $Mn(1)O_6$ octahedra are larger than the $Mn(2)O_6$ ones; this is explained by the strong distortion of the Ba(1)–O(1) layers, with O(1) about 0.21 Å away from the Ba(1) plane (0.22 Å in $Ba_4PrMn_3O_{12}$). Finally, the separation between a $Ba(1)O_3$ layer and a $Ba(2)O_3$ layer is 2.32 Å (2.32 in $Ba_4PrMn_3O_{12}$), also far from the ideal value.

The Mn(1)–Mn(2) distances (2.484 and 2.447 Å, in $Ba_4CeMn_3O_{12}$ and $Ba_4PrMn_3O_{12}$, respectively) agree well with those of similar oxides also containing face-sharing octahedra as 2*H*-$BaMnO_3$ (2.39 Å) [24], $Ba_4Mn_3O_{10}$(2.62 Å) [21] or $Ba_6Mn_5O_{16}$(2.39−2.58 Å) [22].

This scheme of metal–metal distances, besides the presence of lanthanide ions (Ce(IV) or Pr(IV)), should be reflected in the magnetic properties of these materials. Magnetic susceptibility measurements as well as neutron diffraction experiments are in progress and will be the subject of a forthcoming publication.

4. Concluding remarks

Novel 1-D manganites containing rare-earth elements, such as cerium or praseodymium have been prepared. Their structure was determined by combining HREM and XRD, to be that of the 12*R* polytype. An irregular stacking and a severe distortion of the BaO_3 layers are produced to accommodate the large tetravalent lanthanide ions.

HREM revealed the formation, at least at short range, of some other polytypes with different sequences of MnO_6 and REO_6 octahedra.

Acknowledgments

This work was carried out with the financial assistance of CONACYT (Mexico) under Grant 31198U. Financial support form the Comunidad Autónoma de Madrid (Project CAM Expt. 25/2001-CET2001) is gratefully acknowledged.

References

[1] P. Strobel, C. Mouget, Mater. Res. Bull. 28 (1993) 93.
[2] A.R. Armstrong, P.G. Bruce, Nature 381 (1996) 499.
[3] S. Guillement-Fritsch, J.L. Baudow, C. Chanel, F. Bourec, A. Rousset, Solid State Ion. 132 (2000) 63.
[4] Q. Feng, H. Kanoh, K. Ooi, J. Mater. Chem. 9 (1999) 319.
[5] R. von Helmot, J. Wecker, B. Holzapfel, L. Shultz, K. Samwer, Phys. Rev. Lett. 71 (1993) 2331.
[6] Y. Morimoto, A. Asamitsu, H. Kawahara, Y. Tokura, Nature 380 (1996) 141.
[7] J. Vente, K.V. Kamenev, D.A. Sokolov, Phys. Rev. B 64 (2001) 214403.
[8] G.V. Bazuev, V.N. Krasilnikov, D.G. Kellerman, J. Alloys, Compd. 352 (2002) 190.
[9] J.M. González-Calbet, M. Parras, J. Alonso, M. Vallet-Regí, J. Solid State Chem. 111 (1994) 202.
[10] M. Parras, J.M. González-Calbet, J. Alonso, M. Vallet-Regí, J. Solid State Chem. 113 (1994) 78.
[11] N. Créon, C. Michel, M. Hervieu, A. Maignan, B. Raveau, Solid State Sci. 5 (2003) 243.
[12] P.D. Battle, D.E. Cox, M.A. Green, J.E. Millburn, L.E. Spring, P.G. Radaelli, M.J. Rosseinsky, J.F. Vente, Chem. Mater. 9 (1997) 1042.
[13] C.N.R. Rao, A.K. Cheetham, R. Mahesh, Chem. Mater. 8 (1996) 2421.
[14] Y. Doi, M. Wakeshima, Y. Hinatsu, A. Tobo, K. Ahoyama, Y. Yamaguchi, J. Mater. Chem. 11 (2001) 3135.
[15] C. Rabbow, H.K. Mueller-Buschbaum, Z. Naturforsch. 49 B (1994) 1277.
[16] J. Rodriguez-Carvajal, FULLPROF program, in: Abstracts of the Satellite Meeting on Powder Diffraction of the XVth Congress of the IUCr, Toulouse, France, 1990, p. 17.
[17] T. Negas, R.S. Roth, J. Solid State Chem. 3 (1971) 323.
[18] C.H. de Vreugd, H.W. Zandbergeng, J.W. Ijdo, Acta Crystallogr. C 40 (1984) 1987.
[19] K. Boulahya, M. Hernando, A. Varela, J.M. González-Calbet, M. Parras, U. Amador, J.L. Martinez, Eur. J. Inorg. Chem. 4 (2002) 805.
[20] K. Boulahya, M. Hernando, A. Varela, J.M. González-Calbet, M. Parras, U. Amador, Chem. Eur. J. 8 (2002) 4973.
[21] V. Zubkov, A. Tyutyunnik, I.F. Berger, V.I. Voronin, G.V. Bazuev, C.A. Moore, P.D. Battle, J. Solid State Chem. 165 (2002) 454.
[22] K. Boulahya, M. Parras, J.M. González-Calbet, J.L. Martínez, Chem. Mater. 14 (10) (2002) 4006.
[23] R.D. Shannon, Acta Crystallogr. A 32 (1976) 751.
[24] A. Hardy, Acta Crystallogr. 15 (1962) 179.